

Experimental investigation of antigorite dehydration fabrics at high pressure and high temperature

ABSTRACT

Antigorite dehydration is well known as a key process in convergent boundaries for the genesis of mantle wedge partial melting and intermediate-depth earthquakes. However, the crystallographic preferred orientations (CPOs) of prograde minerals from antigorite dehydration and its effects on seismic anisotropy of subducting slabs remain ambiguous and controversial. Here we report hydrostatic dehydration experiments on foliated serpentized peridotite at pressures of 0.3-6 GPa and temperatures of 700-900 °C. Our results show that the orientations of prograde olivine inherit orientations from adjacent olivine grains in the olivine-rich layer by epitaxial growth. In contrast, olivine CPOs evolved with the grain size from the fabric featuring clear [100] point maxima and [001] girdles for fine-grained olivine to orthorhombic patterns characterized by clear [100] and [001] point maxima for coarse-grained olivine, i.e., type-C CPO. We propose that the fine-grained olivine CPO is developed by topotactic growth at the onset of dehydration, while the orthorhombic type-C CPO for the coarse-grained olivine, especially the [001] point maximum along the lineation, is mainly developed by anisotropic growth resulting from anisotropic fluid flow during the dehydration. The developed olivine type-C CPO in the antigorite-rich layer after antigorite dehydration could explain the trench or strike parallel seismic anisotropy observed at convergent plate boundaries.

BACKGROUND

➤ **The debate:** B-type olivine CPO was suggested to form by topotactic growth with the [010]_{ol} parallel to the (001)_{atg} and the [001]_{ol} parallel to the [010]_{atg} in natural samples (Nagaya et al., 2014). However, previous antigorite dehydration experiments show strong CPOs of prograde olivine and enstatite characterized by the [100]_{ol} parallel to the (001)_{atg} from the protolith (Padrón-Navarta et al., 2015). In contrast, TEM observations document that the orientations of crystalline olivine and enstatite nano-grains in partially dehydrated antigorite crystal are randomly distributed (Gualtieri et al., 2012).

➤ **The purpose of this study:** To constrain the crystallographic preferred orientations of prograde minerals from antigorite dehydration and its effects on seismic anisotropy of subducting slabs.

SAMPLES AND RUN PRODUCTS

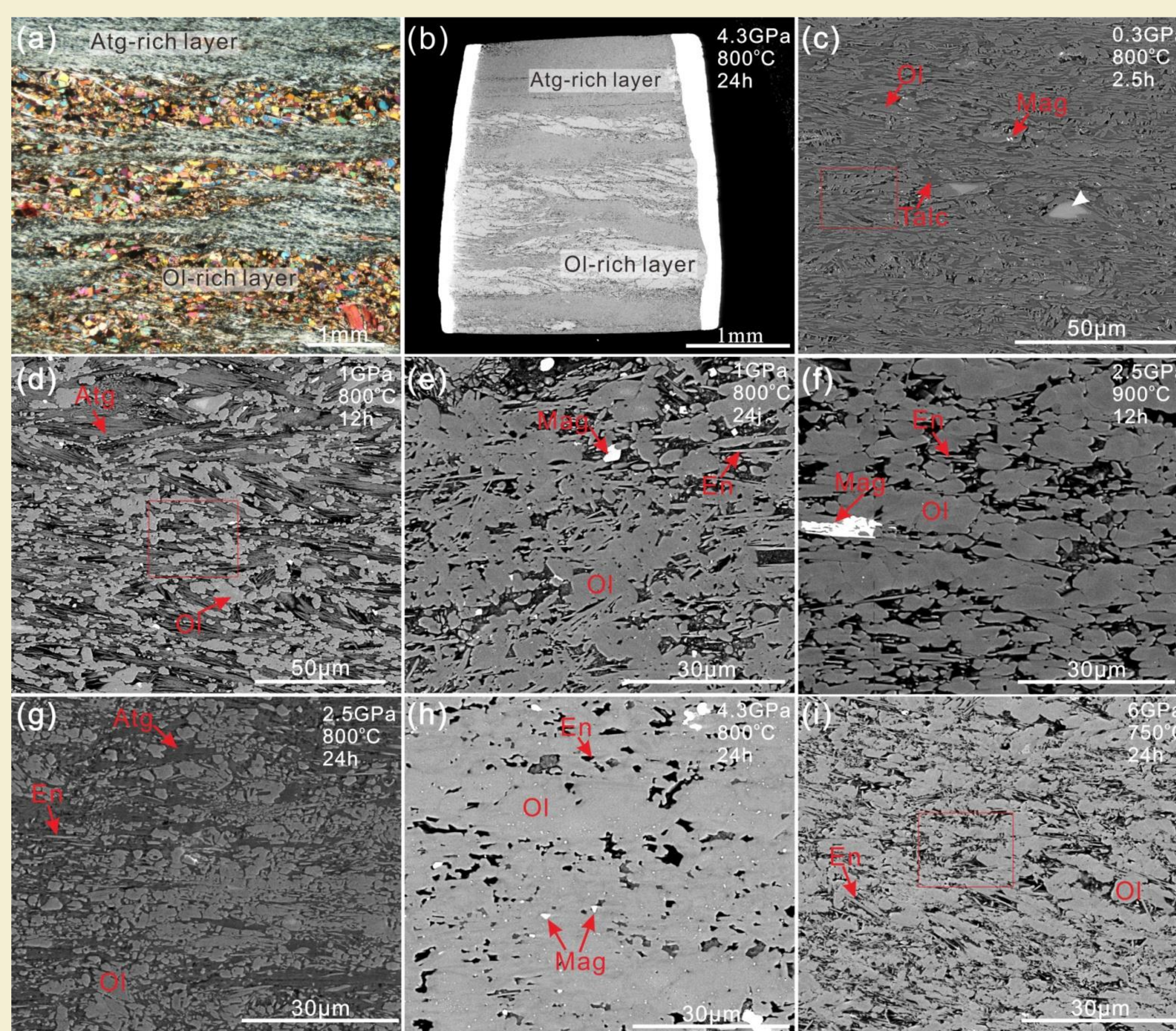


Fig.1. Microstructures of undehydrated starting material (a) and partially or completely dehydrated experimental specimens (b-i). (a) The alternative antigorite-rich layers and olivine-rich layers in starting material. (b) The electron backscattered image of a dehydrated specimen (Sample # R941). (c-f) Dehydration products in antigorite-rich layers under different experimental conditions. The red rectangle boxes in c, d, i are enlarged in figure 3. Atg: antigorite; En: enstatite; Ol: olivine; Mag: magnetite.

Wenlong Liu, Junfeng Zhang, Hongwei Qi and Yongfeng Wang

State Key Laboratory of Geological Processes and Mineral Resources, School of Earth Sciences, China University of Geosciences, Wuhan, Hubei 430074 China

EXPERIMENTAL APPARATUS



EXPERIMENTAL CONDITIONS

Exp. No.	P (GPa)	T (°C)	Duration (hrs)	Grain Size (µm)*		Aspect Ratio*		Products
				Ol	En	Ol	En	
PA328	0.3	700	2.5	2.9	-	6.7	-	Ol+Talc+Atg+H ₂ O
PC383	1	800	24	2.5	1.9	2.6	5.2	Ol+En+H ₂ O
PC372	1	800	12	2.7	2.0	2.7	4.2	Ol+En+Atg+H ₂ O
GA388	2.5	800	24	3.4	2.2	3.2	5.0	Ol+En+Atg+H ₂ O
R925	2.5	900	12	4.7	3.5	3	4.4	Ol+En+H ₂ O
R962	2.5	900	24	5.1	2.5	3.7	5.6	Ol+En+H ₂ O
R941	4.3	800	24	6.3	2.7	2.8	4.1	Ol+En+H ₂ O
R953	4.3	800	2	3.8	3.6	2.6	5.3	Ol+En+H ₂ O
R954	6	750	24	4.9	1.3	3.4	4.0	Ol+En+H ₂ O

DEHYDRATION MICROSTRUCTURES

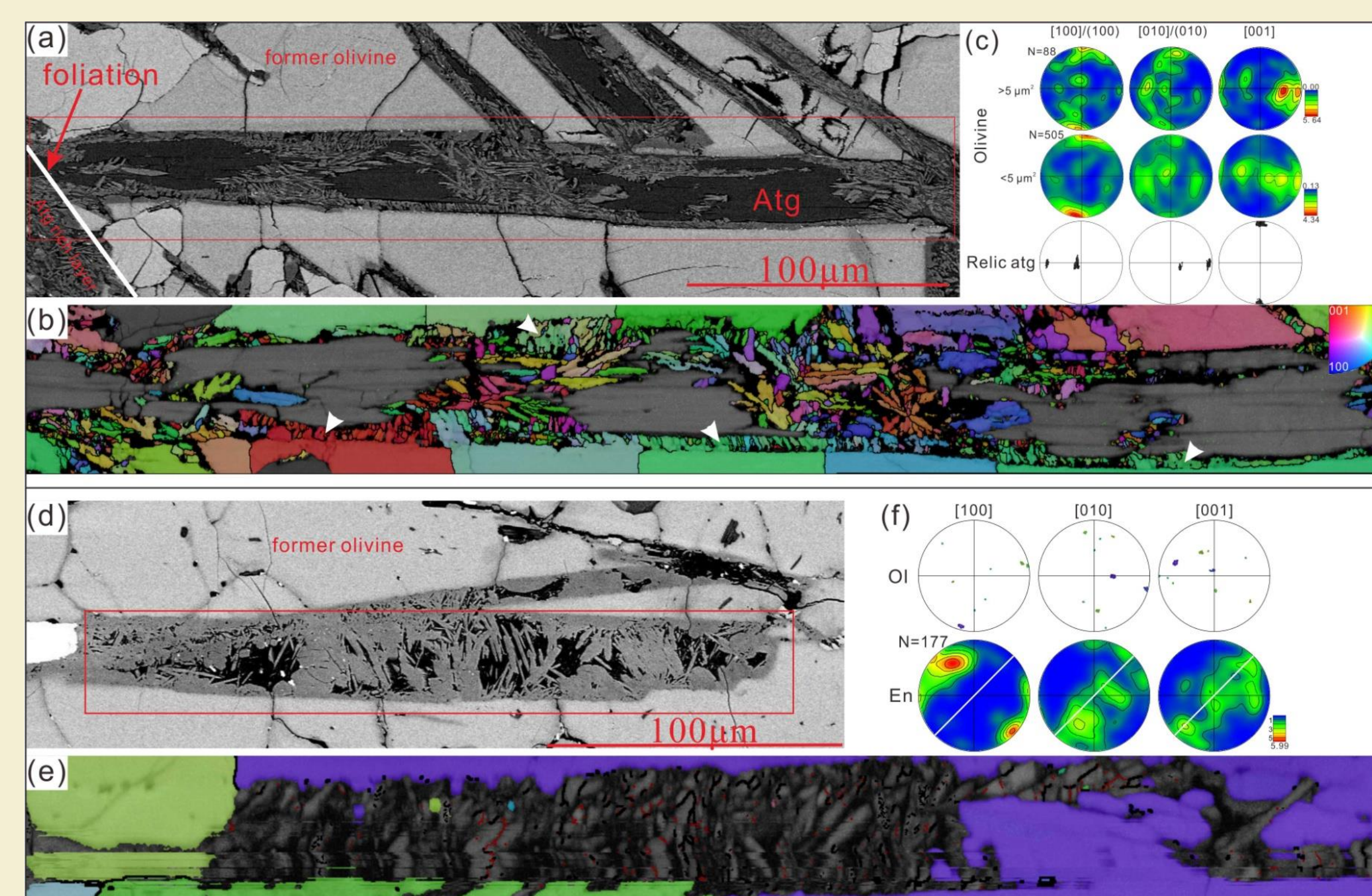


Fig. 2. Microstructure of a partially dehydrated antigorite grain at low pressure (PA328, 0.3 GPa and 700 °C) (a-c) and a completely dehydrated antigorite grain high pressure (PC383, 1 GPa and 800 °C) (d-f) in olivine-rich layer. (a, d) Orientation contrast images. (b, e) Band contrast map overlaid with olivine orientation map colored with inverse pole figure coding. The prograde olivine grains are elongated subparallel to the long axis of antigorite. (c, f) Pole figures of dehydration products (olivine and enstatite) and relic antigorite. It is illustrated in Figure 2c the pole figures of coarse-grained (area >5 µm²) and fine-grained (area <5 µm²) prograde olivine grains in the center of the antigorite without the olivine grains distributed along olivine-antigorite boundary. Figure 2f shows CPO of olivine and enstatite, the white line in the pole figure represents the inferred orientation of the (001) plane of former antigorite.

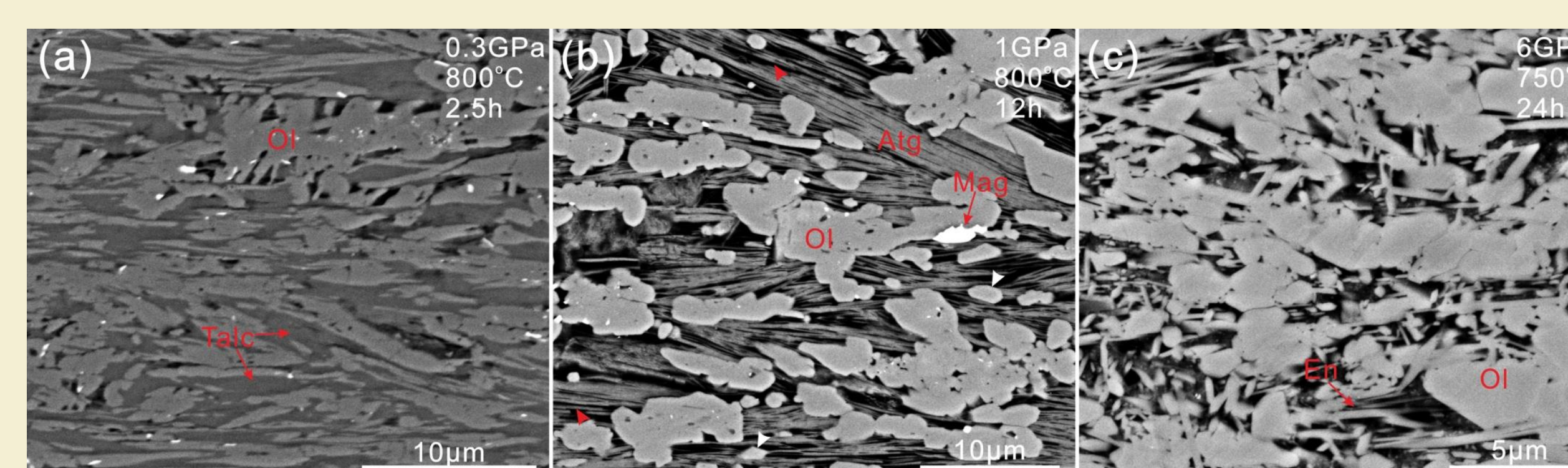


Fig.3. High-magnification microstructures of experimental products in antigorite-rich layers. (a) 0.3GPa, 700 °C (PA328), strongly elongated olivine and talc after completed dehydration (b) 1GPa, 800 °C (PC372), partially dehydrated antigorite. Fiber structure with long axis parallel to lineation is observed. Olivine grains with nanometer size and grains larger than 10 µm is observed. The fine-grained olivine have polygonal shape while coarse grained olivine have serrated shapes. (c) 6GPa, 750 °C (R954), enstatite grains are acicular with long axis subparallel to former lineation.

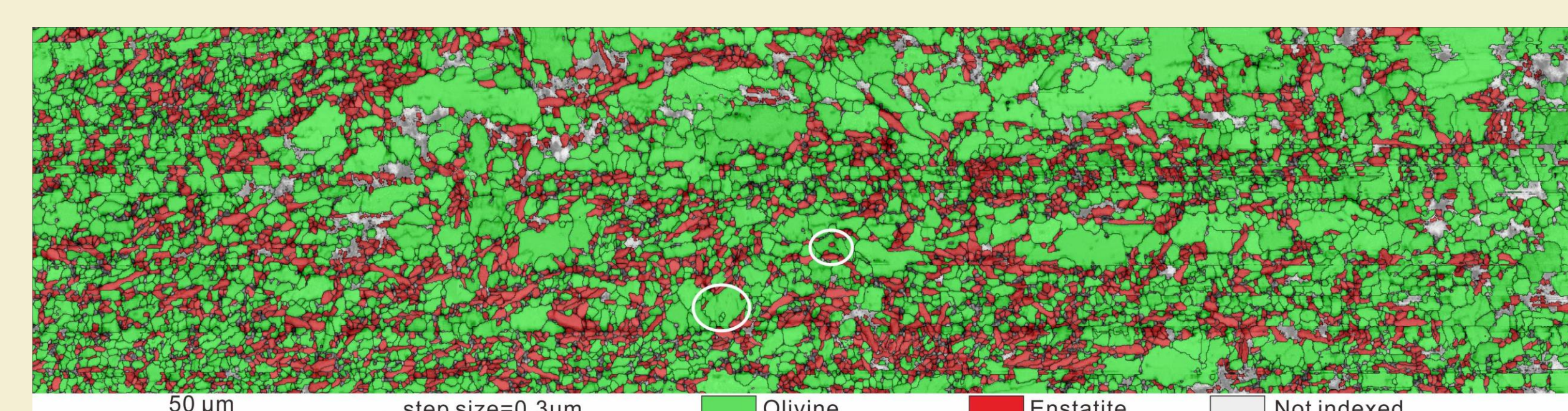


Fig. 4. High-resolution band contrast map overlaid with phase map of R941 in the antigorite rich layer (0.3µm). The green and red color represent olivine and enstatite, respectively. The open ellipses mark olivine and enstatite inclusions in coarse grained olivine.

DEHYDRATION FABRICS

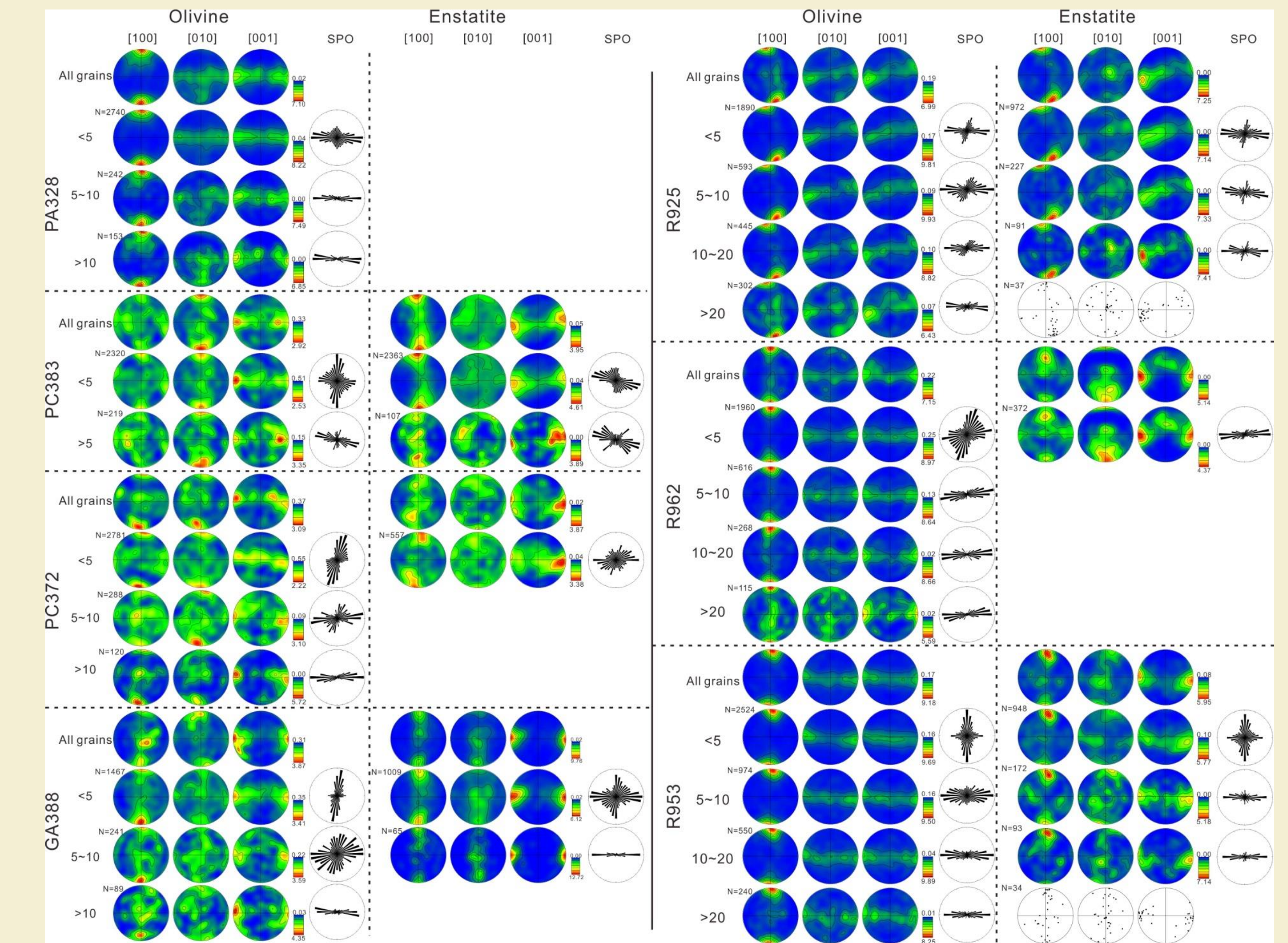


Fig. 5. The evolution of CPOs and SPOs of prograde minerals (olivine and enstatite) with grain size (in area).

FABRIC STRENGTH

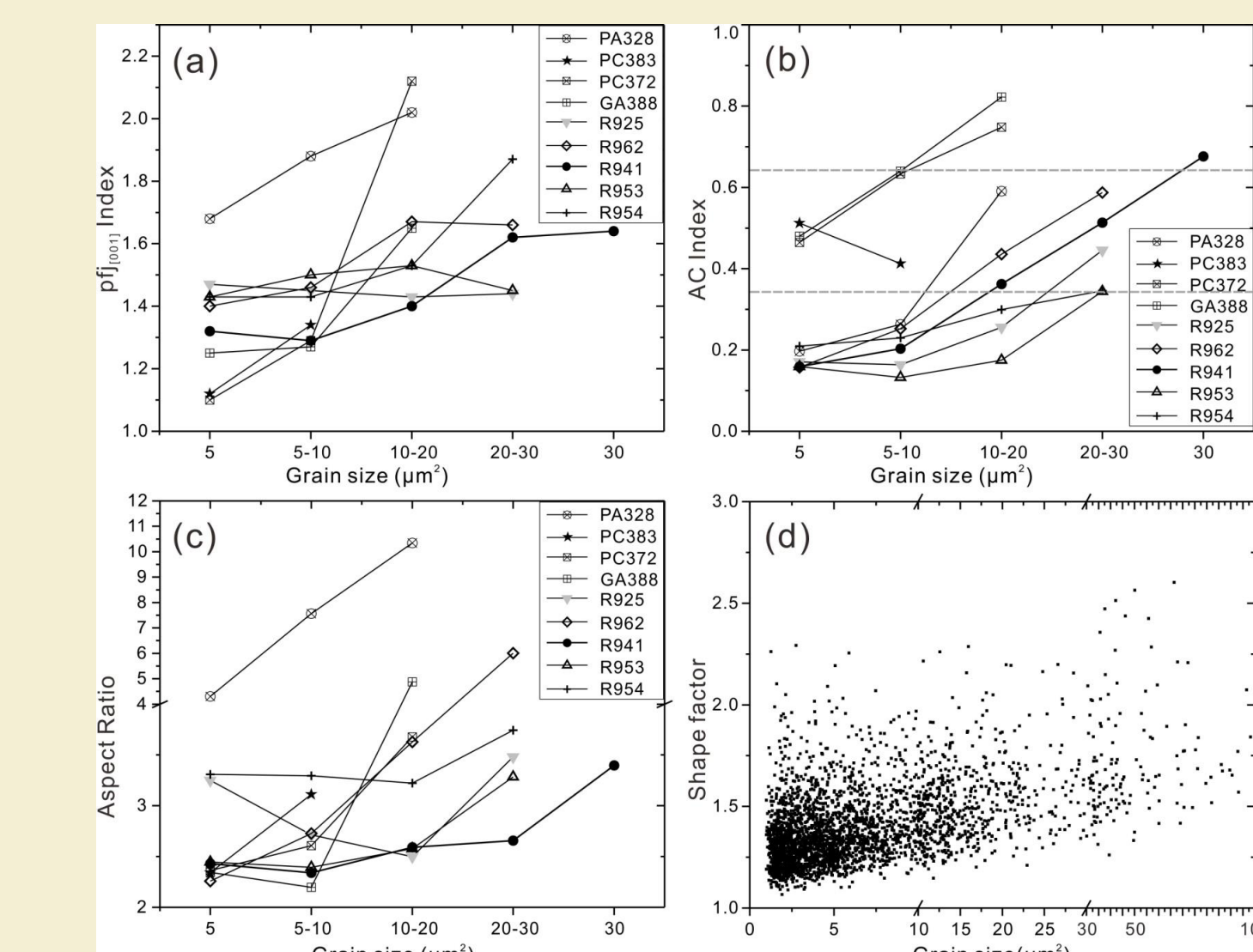


Fig. 6. The plots of fabric strength (a), CPO symmetry (b), area averaged aspect ratio (c) and shape factor (d) versus grain size in antigorite-rich layers. The variation in olivine CPO symmetry as a function of the AC index in figure 5b is illustrated on the right of the diagram. The shape factor which is the ratio between the actual perimeter of the grain and the perimeter of a circle with the same area quantifies the sinuosity of grain shape.

SEISMIC PROPERTIES

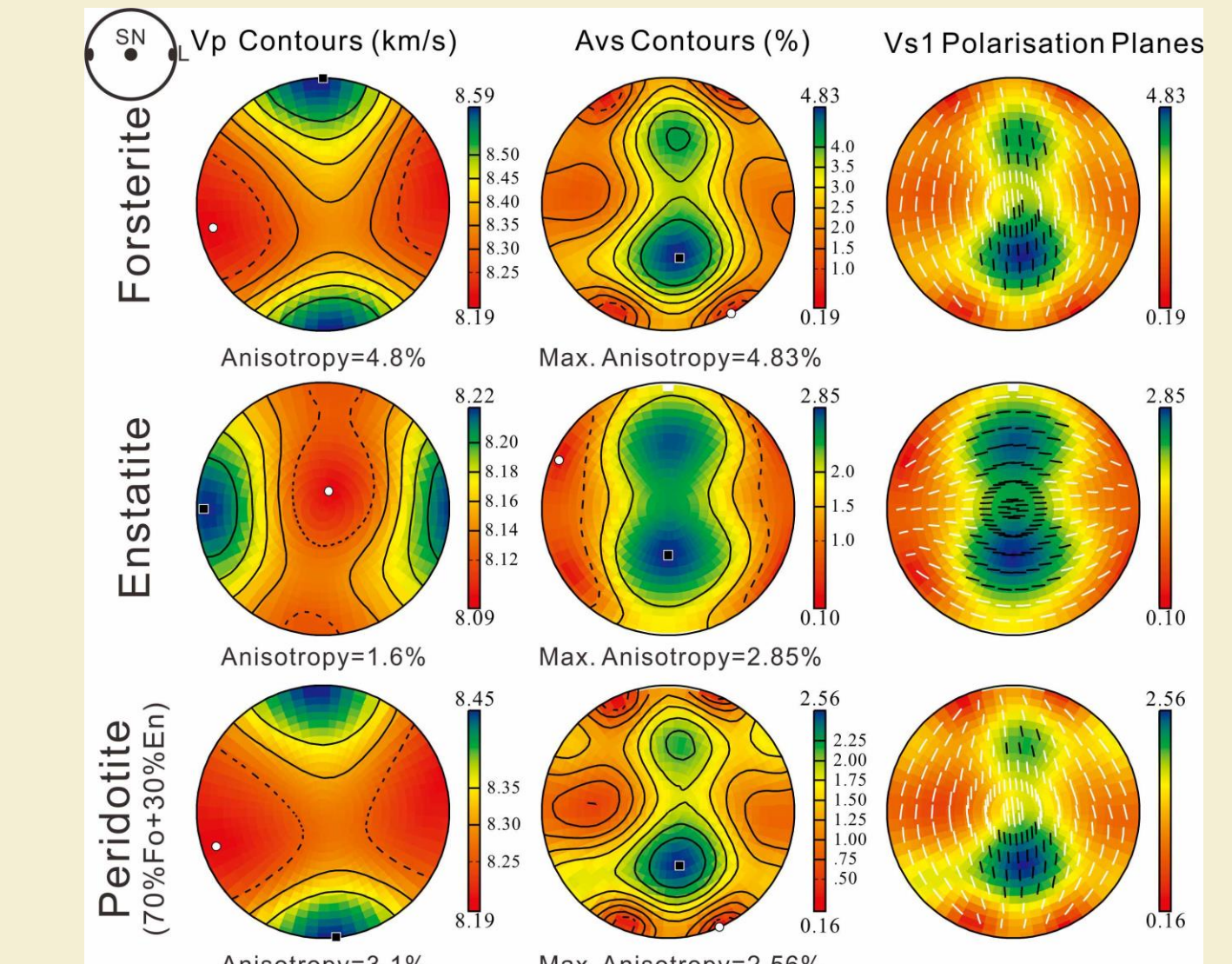


Fig. 7. Calculated seismic properties of prograde olivine, enstatite and peridotite from an antigorite-rich layer based on the EBSD data of specimen#R941. The seismic properties of peridotite are calculated based on modal proportions of 30% enstatite and 70% olivine. SN: foliation normal, L: lineation.

CONCLUSIONS

- The orientations of prograde olivine inherit orientations from adjacent olivine grains in the olivine-rich layer by epitaxial growth. In contrast, olivine CPOs evolved with the grain size from the fabric featuring clear [100] and [001] point maxima for fine-grained olivine to orthorhombic patterns characterized by clear [100] and [001] point maxima for coarse-grained olivine, i.e., type-C CPO.
- Our experimental results document for the first time that olivine type-C CPOs can result from both topotactic growth and anisotropic growth imposed by the anisotropic fluid pressure gradient.
- The prograde minerals from antigorite dehydration could contribute to the trench- or strike-parallel polarization of the faster shear wave in convergent boundaries.

REFERENCES

[1] Gualtieri, A. F., Giacobbe, C., Viti, C. (2012). The dehydroxylation of serpentine group minerals. *American Mineralogist*, 97(4), 666-680. <https://doi.org/10.2138/am.2012.3952>

[2] Nagaya, T., Wallis, S. R., Kobayashi, H., Michibayashi, K., Mizukami, T., Seto, Y., Miyake, A., Matsumoto, M. (2014). Dehydration breakdown of antigorite and the formation of B-type olivine CPO. *Earth and Planetary Science Letters*, 387, 67-76. <https://doi.org/10.1016/j.epsl.2013.11.025>

[3] Padrón-Navarta, J. A., Tommasi, A., Garrido, C. J., Mainprice, D. (2015). On topotaxy and compaction during antigorite and chlorite dehydration: an experimental and natural study. *Contributions to Mineralogy and Petrology*, 169(4). <https://doi.org/10.1007/s00410-015-1129-4>